Desalination and Water Treatment
www.deswater.com

doi: 10.5004/dwt.2017.20846

77 (2017) 264–273
May

Removal of chlorite from aqueous solution by MIEX resin

Lei Ding[a,b,*], Yunhua Zhu[c], Xiaopeng Jin[a], Jiangya Ma[a,b], Xinxi Zhang[a,b], Jan Peter van der Hoek[d,e]

[a]*School of Civil Engineering and Architecture, Anhui University of Technology, 59 Hudong Road, Maanshan 243002, China, emails: dinglei1978@163.com (L. Ding), 18355512810m0@sina.cn (X. Jin), majiang_ya@126.com (J. Ma), zhang-xinxi@163.com (X. Zhang)*
[b]*Engineering Research Center of Biomembrane Water Purification and Utilization Technology Ministry of Education, Anhui University of Technology, 59 Hudong Road, Maanshan 243002, China*
[c]*School of Energy and Environment, Anhui University of Technology, 59 Hudong Road, Maanshan 243002, China, email: zhuchem01@163.com*
[d]*Department of Water Management, Faculty of Civil Engineering and Geosciences, Delft University of Technology, P.O. Box 5048, 2600 GA, Delft, The Netherlands, email: j.p.vanderhoek@tudelft.nl*
[e]*Strategic Centre, Waternet, Korte Ouderkerkerdijk 7, 1096 AC Amsterdam, The Netherlands*

Received 8 September 2016; Accepted 24 April 2017

ABSTRACT

This research investigates the feasibility of magnetic ion exchange (MIEX) resin as the adsorbent for the removal of chlorite through a laboratory study using batch adsorption experiments. The agitation speed of 100 rpm is the optimum agitation intensity. The removal efficiency of chlorite increases with increasing dosage of MIEX resin. The optimum pH is 5–7. The coexisting anions and natural organic matter reduce the removal efficiency of chlorite. The kinetic process at the low chlorite concentration (1.02 mg/L) is highly possible to be pseudo-first-order. However, the pseudo-second-order model can fit the kinetic data quite well at higher chlorite concentrations (2.28–5.57 mg/L). At the initial stage of adsorption, the intra-particle diffusion is the rate-limiting step, but the adsorption rate is controlled by the film diffusion and the intra-particle diffusion after 10 min. The adsorption equilibrium can be approximately attained within 40 min, and Redlich–Peterson isotherm model fits best to the equilibrium data. The adsorption is a thermodynamically feasible, spontaneous, and endothermic ion-exchange process. The removal of chloride on MIEX resin is an ion-exchange mechanism. Dissolved organic carbon can be removed effectively as well as chlorite and chlorate using MIEX resin in real water. Therefore, MIEX resin is a promising technology for the removal of chlorite from aqueous solution.

Keywords: Adsorption; Chlorite; Ion exchange; Kinetics; MIEX resin

1. Introduction

Chlorine dioxide (ClO_2) is used extensively as an oxidant/disinfectant for removing color and algae, controlling taste and odor, and inactivating virus, bacteria, and protozoan pathogens [1]. Particularly, pre-oxidation with chlorine dioxide before chlorination disinfection during drinking water treatment can significantly decrease the levels of chlorinated and halogenated organic by-products, such as trihalomethanes and haloacetic acids [2]. However, the undesired inorganic by-product, chlorite (ClO_2^-), is generated (approximately 50%–70% of chlorine dioxide consumed by oxidation reaction is converted into chlorite during the pre-oxidation) [3,4]. Toxicological tests conducted in animals demonstrate that chlorite may cause the hematological damage [4,5]. It is also reported that chlorite causes adverse effects on reproduction and development of tested animals, such as abnormal pups, low brain weight, low birth weight, and retardation in the sexual development in males and females [6–8]. Based

---

[*] Corresponding author.

on the health concerns over chlorite, the US Environmental Protection Agency (USEPA) proposes a maximum contaminant level of 1.0 mg/L of chlorite in drinking water, while the World Health Organization (WHO) Guidelines show the limited concentration of chlorite is 0.70 mg/L [9,10]. In the new Chinese Sanitary Standards for Drinking Water (GB 5749-2006), it has been regulated at the threshold value of 0.70 mg/L for chlorite. However, according to the survey conducted by Ministry of Health of People's Republic of China in 2011, the chlorite concentration in the finished drinking water from 19 drinking water treatment plants is more than 0.70 mg/L among the 25 investigated drinking water treatment plants using chlorine dioxide as pre-oxidant in a city located in south China, and even, the maximum value of chlorite concentration is 2.20 mg/L [11]. Therefore, finding an efficient method for the removal of chlorite is necessary for improving the potential use of chlorine dioxide in drinking water treatment.

Many experiments have been conducted to find efficient methods for removing chlorite. The excess sulfur dioxide–sulfite ion can effectively remove chlorite from aqueous solution at a pH range of 5–7, but the free chlorine has to be used to clean the remaining excess sulfur dioxide and sulfite ions [12]. In addition, in the presence of dissolved oxygen in aqueous solution, sulfur dioxide can oxidize the chlorite into chlorate which has also negative effect on health [13,14]. Ferrous ion can remove chlorite fast and effectively by reducing chlorite to chloride at a pH range of 5–7, but additional dosage of ferrous ions is required because of the consumption of oxygen for ferrous ion oxidation under the conditions of high pH (pH > 7) and high oxygen concentration in aqueous solution [15]. Chlorite can be removed on the surface of activated carbon by adsorption and chemical reduction at pH < 7, but the removal efficiency decreases rapidly below 30% with the increase in time and pH [3,12]. Li et al. [16] investigated the removal of chlorite and chlorate adsorbed on calcium carbonate, but the removal efficiency of chlorite is only around 30%. As an anion in aqueous solution, probably chlorite can be removed by anion-exchange resin. But, to our knowledge, up to now, there is no related report about the removal of chlorite with anion-exchange resins. Therefore, magnetic ion exchange (MIEX) resin, as a novel strong-basic anion resin, may be a potential candidate as an adsorbent for the removal of chlorite from aqueous solution.

MIEX resin, manufactured by Orica Watercare, is a magnetically enhanced, macro-porous anion-exchange resin with quaternary ammonium functional groups and chloride ion as an exchangeable ion [17,18]. The theoretical exchange capacity of MIEX resin is 0.52 mmol/mL [19]. Compared with traditional anion-exchange resins [20], the iron oxide (γ-Fe_2O_3) incorporated into the polyacrylic matrix during the preparation of resin facilitates the rapid aggregation and settling of MIEX resin after adsorption, allowing the resin beads to be smaller [21]. The average size of MIEX resin is 180 μm in diameter (2–5 times smaller than traditional ion-exchange resin), which makes MIEX resin possess larger specific surface area that allow a fast adsorption rate [22]. Owing to the smaller size, MIEX resin can be used in a slurry form, and mixed well with adsorbate by mechanical stirring with a low agitation intensity, thus decreasing the resistance of solid–liquid phase mass transfer [23]. The saturated resins can be regenerated effectively using brine. For MIEX resin, most researches were focused on the pre-treatment stage before conventional drinking water treatment processes for NOM removal [24], micro-pollutants removal [25,26], decreasing the dosage of coagulant and ozone [22,27], and controlling membrane fouling [28]. During the pre-treatment of raw water from different water sources, many researchers found that MIEX resin can remove inorganic anions such as bromide, sulfate, nitrate, and perchlorate [29–32]. However, as far as we know, until now, there is no report with respect to the removal of chlorite by MIEX resin. Particularly, MIEX resin has not yet been used to remove chlorite after sedimentation and before filtration processes in the drinking water treatment plants where chlorine dioxide is used as an oxidant to pre-oxidize raw water. Doing so enhances the security of chlorine dioxide use in drinking water treatment.

Accordingly, the objective of this study was to evaluate the potential of MIEX resin as an adsorbent for the removal of chlorite from aqueous solution through a laboratory study using batch adsorption experiments. Factors affecting the removal of chlorite were investigated. Adsorption equilibrium and kinetics equations were established to quantitatively describe the adsorption behavior. The thermodynamic parameters were calculated. The removal mechanism of chlorite was confirmed. Finally, three real water samples were used to evaluate the removal efficacy of chlorite MIEX resin.

2. Materials and methods

2.1. Materials

MIEX resin, supplied by Beijing Sino-Australia Orica Watercare Technology & Equipment Co., Ltd. (Beijing, China) was used as adsorbent in this study. For the surface characterization of MIEX resin such as specific surface area, pore structure, and functional groups, we cannot give any information because these properties are not allowed as a patented product. Before used, the resin was rinsed repeatedly with ultra-pure water to remove fines and impurities and then stored in the ultra-pure water. A certain volume resin used in adsorption can be taken out from the washed resin according to the description in literature [33].

2.2. Chemicals and adsorbate

All chemicals except sodium chlorite were guaranteed reagent grade. Sodium chlorite was used as an adsorbate and the standard stock solution of chlorite (1,000 mg/L) was purchased from ANPEL Scientific Instrument Co., Ltd, Shanghai. Other chemicals were purchased from Sinopharm Chemical Reagent Co., Ltd., China. The samples for a calibration curve were prepared by diluting standard stock solution with ultra-pure water obtained from Millipore Super-Q plus water system. Tested samples in adsorption experiments were prepared by dissolving weighed amount of sodium chlorite (about 82% purity) in desired concentrations with ultra-pure water, and the accurate concentration of chlorite was given by the determination.

2.3. Methods

2.3.1. Equilibrium studies

Equilibrium batch experiments were undertaken at 293, 313, and 333 K, respectively. A set of sealed glass jars containing 0.5 mL MIEX resin and 500 mL of chlorite solution with various initial concentrations (1.0–7.0 mg/L) were kept on the digital display stable temperature magnetic stirrer (78HW-1). The slurries were magnetically stirred at an agitation speed of 100 rpm for 90 min. Then the slurries were filtrated using a filter with a 0.45 μm Millipore membrane. The chlorite remaining in filtrates was determined. Each assay was carried out in triplicate under the same condition and the average values were reported herein. The equilibrium capacity of chlorite adsorbed on MIEX resin at equilibrium, q_e (mg/mL), was calculated by Eq. (1):

$$q_e = \frac{(C_0 - C_e)V}{W} \tag{1}$$

where C_0 and C_e are the liquid-phase concentrations of chlorite (mg/L) at initial and equilibrium, respectively. V (L) is the volume of solution and W (mL) represents the volume of the MIEX resin.

2.3.2. Kinetic studies

Batch kinetic experiments were conducted at various initial chlorite concentrations (1.02, 2.28, and 5.57 mg/L), respectively. The procedures were approximately identical to those of equilibrium studies. The difference was that the water samples were taken from the magnetic stirrer at preset time intervals (5, 10, 20, 30, 40, 50, 60, 70, 80, and 90 min). The amount of chlorite adsorbed on MIEX resin at time t, q_t (mg/mL), was calculated by Eq. (2):

$$q_t = \frac{(C_0 - C_t)V}{W} \tag{2}$$

where C_t is the liquid-phase concentration of chlorite at time t.

2.3.3. Effects of adsorption parameters

The procedures were approximately identical to those of equilibrium studies. The adsorption time is 90 min. A series of tests were performed to investigate the effects of agitation speed, adsorbent dosage, and solution pH on the removal of chlorite by varying agitation intensity from 50 to 300 rpm, varying MIEX resin dosage from 0.5 to 4.0 mL/L, and varying solution pH from 5 to 9. The pH of solution was adjusted by adding 0.10 M HCl or 0.10 M NaOH solutions when necessary. Based on the water qualities of effluents from sedimentation tanks in three drinking water treatment plants, the effects of other anions and natural organic matter were explored by adding chloride (10.0 mg/L), sulfate (10.0 mg/L), chlorate (1.0 mg/L), bicarbonate (10.0 mg/L), and humic acid (DOC = 6.20 mg/L) into chlorite solution with a concentration of 2.10 mg/L, respectively. The removal efficiency of chlorite, E (%), was calculated by the changes of chlorite concentration in liquid-phase.

2.3.4. Analytical measurements

The pH of solution was measured using a pH meter (pHS-3C model, Leici, China). Chlorite was measured on a Shimadu Ion Chromatograph (Shimadu, Japan) with a suppressed conductivity detection. IC SI-52G column (4.6 mm × 10 mm, Shodex, Japan) was used as guard column and an IC SI-52 4E analytical column (4.0 mm × 250 mm, Shodex, Japan) was used to determine the concentration of chlorite. The 3.6 mM sodium carbonate (Na_2CO_3) was used as solvent and the flow rate of the solvent was 0.8 mL/min with a sample injection volume of 20 μL. The temperature of the column and detector compartment was set to 318 K.

2.3.5. Evaluation of isotherm and kinetic models

All the model parameters were evaluated by non-linear regression using OriginPro 8.5 software (OriginLab Corporation, USA). Correlation coefficient (R^2) and the standard error (SE) were used to evaluate the validity of models. The higher R^2 and smaller SE indicate a better fit to the experiment data. The values of SE can be calculated by Eq. (3) [34]:

$$\text{SE} = \sqrt{\frac{1}{m-p}\sum_{i=1}^{m}(q_{\text{cal}} - q_{\text{exp}})_i^2} \tag{3}$$

where q_{exp} is the experiment data, q_{cal} is the calculated data obtained from the models, m is the number of the experiment data, and p is the number of parameters in the regression model.

3. Results and discussion

3.1. Effect of agitation intensity

Different from the conventional resin usually filled with fixed adsorption units, MIEX resin is generally used in a completely mixed reactor by mechanical agitation. Therefore, the appropriate agitation intensity is greatly significant for dispersing MIEX resin particles into aqueous solution completely and reducing the energy consumption to the utmost extent. Fig. 1 illustrates the agitation speed of 100 rpm is the optimum agitation intensity because the removal efficiency of chlorite basically keeps constant around 80% with increasing agitation speed from 100 to 300 rpm. Hence, the agitation speed of 100 rpm is used in the subsequent adsorption tests. Hsu and Singer [29] also used the agitation speed of 100 rpm in their study about the removal of bromide and natural matter by MIEX resin.

3.2. Effect of MIEX resin dosage

For an adsorption system given initial concentration of pollutant, adsorbent dosage is an important parameter, and needs to be optimized because the usage of optimum dosage can save greatly cost as well as the efficient removal of pollutant. The results, given in Fig. 2, show that the removal efficiency of chlorite increases rapidly from 71.39% to 81.75% with an increase in MIEX resin dosage from 0.50 to 1.0 mg/L, which results from the increased surface area and more available active sites for ion exchange [35]. However, the removal percentage of chlorite has no obvious increase with further increasing dosage from 1.0 to 4.0 mg/L. This may be attributed to the aggregation of resin particles at a high dosage leading to decrease in available adsorption sites and an increase in diffusion path length [36]. Similar results were reported for the removal of bromide on MIEX resin [33].

3.3. Effect of initial pH of solution

The initial pH of solution is a pre-dominant parameter for the adsorption system. It affects the degree of ionization

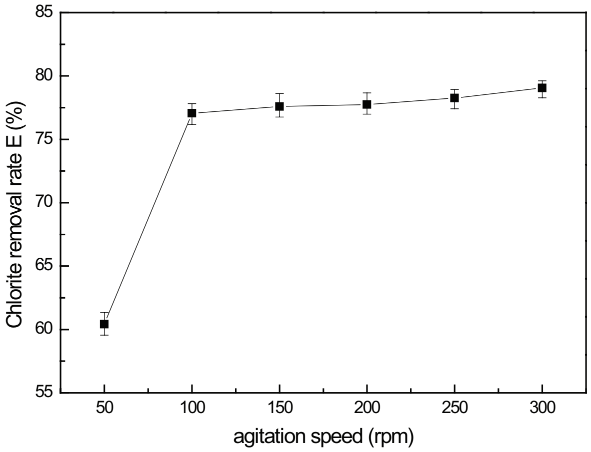

Fig. 1. Effect of agitation speed on the removal of chlorite (the initial chlorite concentration = 2.28 mg/L; adsorbent dosage = 1.0 mL/L; temperature = 290 K; pH without any adjustment; adsorption time = 90 min).

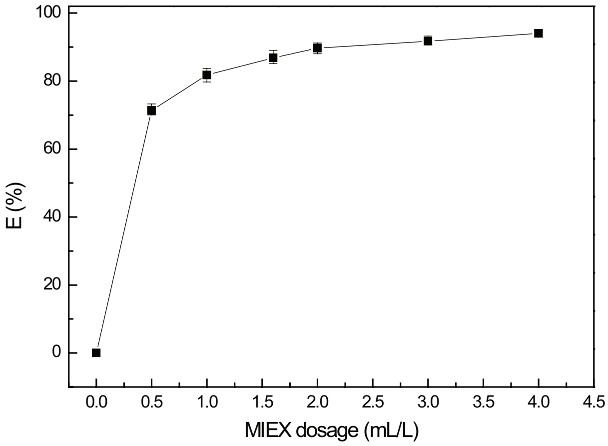

Fig. 2. Effect of adsorbent dosage on the removal of chlorite (the initial chlorite concentration = 2.28 mg/L; agitation speed = 100 rpm; temperature = 290 K; pH without any adjustment; adsorption time = 90 min).

of adsorbate and the surface charge of a solid adsorbent [37]. Owing to the pH of raw water ranging from 6 to 9, tests were conducted to investigate the effects of pH on chlorite removal by varying the initial pH of solution from 5 to 9. The results are shown in Fig. 3. It is shown that the removal percentage of chlorite is relatively high (around 80%) at a pH range of 5–7 although it decreases slightly with an increase in pH. The point of zero charge – pH_{pzc} (measured in this study) of MIEX resin is 6.05. The more negative charges on the surface of MIEX resin may be a reason causing the slight decrease in removal efficiency with increasing pH from 5 to 7 [38]. With increasing pH to 9, the removal efficiency of chlorite decreases rapidly to 38.14%. This may be attributed to the hydroxyl irons competing with chlorite for the adsorption sites. The pH of solution after adsorption is found to decrease from 9 to 7.36, further verifying some hydroxyl ions adsorbed on MIEX resin. The similar competition adsorption was also found for bromide removal using MIEX resin [33].

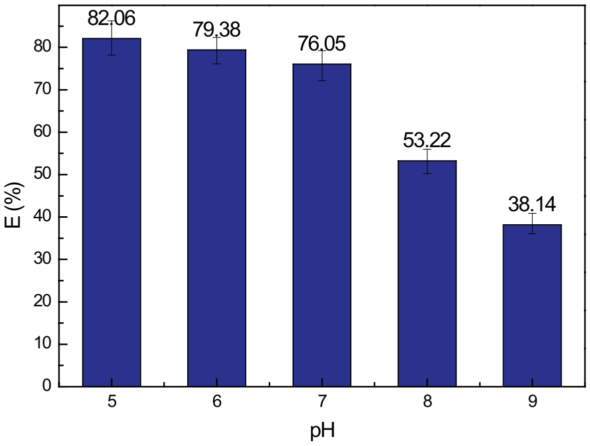

Fig. 3. Effect of initial pH of solution on the removal of chlorite (the initial chlorite concentration = 2.28 mg/L; adsorbent dosage = 1.0 mL/L; agitation speed = 100 rpm; temperature = 290 K; adsorption time = 90 min).

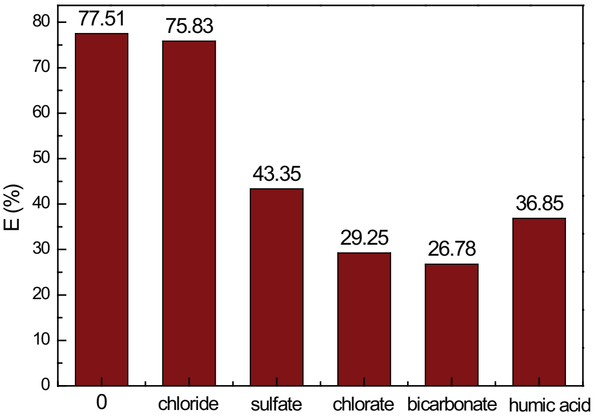

Fig. 4. Effect of coexisting anions and NOM on the removal of chlorite on MIEX resin (the initial chlorite concentration = 2.10 mg/L; adsorbent dosage = 1.0 mL/L; agitation speed = 100 rpm; temperature = 290 K; adsorption time = 90 min).

3.4. Effect of coexisting anions and NOM

After pre-oxidation with chlorine dioxide, coexisting anions and NOM such as chloride, sulfate, bicarbonate, chlorate, and humic acid are usually found as well as chlorite in effluent from sedimentation tank. The effect of these anions and NOM on the removal of chlorite is presented in Fig. 4. Fig. 4 reflects that the coexisting substances have substantially negative effect on the removal of chlorite except chloride. This indicates that these coexisting anions and NOM can compete with chlorite for active sites, decreasing the removal efficiency of chlorite. Similar adverse effects were reported during the removal of bromide and perchlorate using MIEX resin [30,33]. Therefore, more MIEX resin dosage should be used in order to remove chlorite effectively when other anions and NOM with high concentration exist in raw water.

3.5. Adsorption kinetics

Effects of contact time and initial chlorite concentration on the removal of chlorite are shown in Fig. 5. It can be seen clearly from Fig. 5 that the amount of chlorite adsorbed on MIEX resin dramatically increases with an increase in contact time within the first 10 min. This can be interpreted by the fact that a large number of vacant adsorption sites are available during the first 10 min, leading to the rapid adsorption of chlorite on exterior surface of MIEX resin. For the second stage of 10–40 min, the adsorption rate becomes much slower because the slope of the curve is smaller compared to the first stage. This may be due to the reduction of available adsorption sites and the slower diffusion because of the smaller concentration gradient and the repulsive forces of chlorite ions between adsorbed on MIEX resin and in solution [39]. For the third stage after 40 min, the adsorption reaches equilibrium because the curves tend to be flat. Based on above findings, the time needed to attain adsorption equilibrium is about 40 min. This may be attributed to the smaller size of MIEX resin particles. The fast adsorption behavior was also observed during the adsorption of other anions and organic matter on MIEX resin [26,30,33,40]. On increasing the initial chlorite concentration from 1.02 to 5.57 mg/L, Fig. 5 demonstrates that the amount of chlorite adsorbed on MIEX resin also increases. This may be mainly because the greater concentration gradient of chlorite in a high initial chlorite concentration drives the chlorite into the internal pores of MIEX resin, making the internal active sites be used effectively [41].

Quantitatively describing the kinetics of chlorite adsorbed on MIEX resin contributes to the design of adsorption equipment. The pseudo-first-order and pseudo-second-order kinetic models (expressed by Eqs. (4) and (5)) [42,43] were used to fit the kinetic data of chlorite adsorbed on MIEX at different initial chlorite concentrations in this study, respectively. And the fitted results are presented in Table 1.

$$q_t = q_e(1 + e^{-k_1 t}) \tag{4}$$

$$q_t = k_2 q_e^2 t / (1 + k_2 q_e t) \tag{5}$$

where t (min) is adsorption time; k_1 (1/min) and k_2 (mL/mg min) are the rate constant of pseudo-first-order and pseudo-second-order kinetic models, respectively.

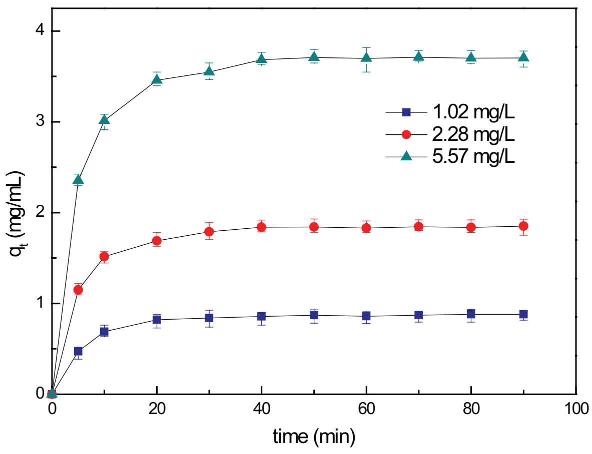

Fig. 5. Effect of contact time and initial chlorite concentration on the removal of chlorite (adsorbent dosage = 1.0 mL/L; agitation speed = 100 rpm; temperature = 290 K; pH without any adjustment).

Table 1
Kinetic parameters for the removal of chlorite adsorbed on MIEX resin

		Pseudo-first-order model				Pseudo-second-order model				Intra-particle diffusion model					
C_0 (mg/L)	$q_{e,exp}$ (mg/mL)	$q_{e,cal}$ (mg/mL)	k_1 (1/min)	R^2	SE	$q_{e,cal}$ (mg/mL)	k_2 (mL/mg min)	R^2	SE	k_{id1} (mg/mL min$^{1/2}$)	R^2	k_{id2} (mg/mL min$^{1/2}$)	R^2	k_{id3} (mg/mL min$^{1/2}$)	R^2
1.02	0.88	0.87	0.1573	0.9937	0.13	0.93	0.2810	0.9594	0.33	0.215	0.999	0.019	0.999	0.005	0.9344
2.28	1.85	1.83	0.1885	0.9715	0.68	1.94	0.1608	0.9826	0.53	0.493	0.9959	0.080	0.9747	0.004	0.9854
5.57	3.70	3.66	0.1908	0.9704	1.05	3.90	0.0832	0.9873	0.69	1.009	0.9917	0.123	0.974	0.004	0.9610

Table 1 shows that compared with the pseudo-second-order model, at the low chlorite concentration (1.02 mg/L), the value of correlation coefficient ($R^2 = 0.9937$) of pseudo-first-order model is distinctly higher, and its SE = 0.12 is also lower. Accordingly, the kinetic process of chlorite adsorbed on MIEX resin at the low chlorite concentration is highly possible to be pseudo-second-order. The pseudo-first-order model is based on the film diffusion theory and it is usually suitable to describe the rapid adsorption process [44]. At low chlorite concentration, the active sites of MIEX resin are so sufficient that the chlorite can be quickly adsorbed on the exterior surface of MIEX resin. Indeed, Fig. 5 also demonstrates the adsorption rate is very fast (approximately reaching equilibrium within 20 min) at the low concentration. This may be the reason why the pseudo-second-order model gives a good simulation. Conversely, the pseudo-second-order model can fit the kinetic data quite well at higher chlorite concentrations (2.28 and 5.57 mg/L) with higher R^2 and lower SE values.

Generally, the adsorption rate is controlled by film diffusion or/and intra-particle diffusion. The rate-controlling step was analyzed by fitting the kinetics data of chlorite adsorbed on MIEX resin using the intra-particle diffusion model expressed by Eq. (6) [45]:

$$q_t = k_{\mathrm{id}} t^{1/2} + C_i \tag{6}$$

where k_{id} (mg/mL min$^{1/2}$) is the intra-particle diffusion rate constant, and C_i is the intercept related to the boundary layer effect.

Based on the intra-particle diffusion theory proposed by Weber and Morris [45], the plot of q_t vs. $t^{1/2}$ will be linear and pass through the origin if the intra-particle diffusion is the only rate-controlling step. Otherwise, the film diffusion may be also involved as well as the intra-particle diffusion [41]. The plots of q_t vs. $t^{1/2}$, shown in Fig. 6, are not linear within the whole adsorption time but multi-linear. For the first portion, the linear plots all approximately pass through the origin, revealing the intra-particle diffusion is the only rate-controlling step and controls the initial adsorption rate of chlorite on MIEX resin. This may be due to the fact that the initial chlorite concentration is higher, making the film diffusion (external diffusion) fast. For the second portion, the plots do not pass through the origin and the intercepts exist, suggesting that both the film diffusion and the intra-particle diffusion control the adsorption rate. This is because the liquid film diffusion becomes slow with the chlorite concentration gradient decreasing gradually in this stage. The third portion means the equilibrium stage where the intra-particle diffusion starts to slow down due to the extremely low chlorite concentration.

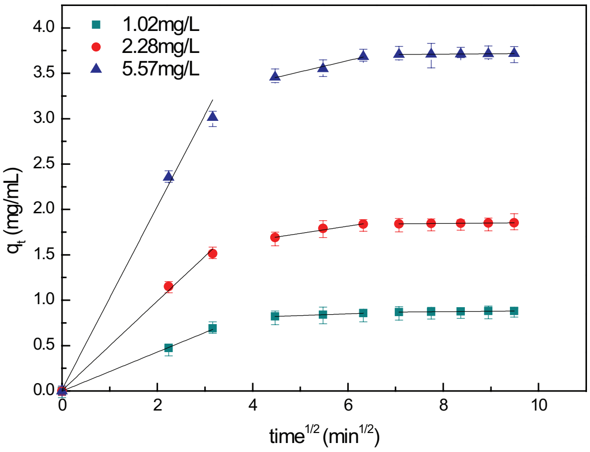

Fig. 6. Plots of intra-particle diffusion model for the adsorption of chlorite on MIEX resin.

3.6. Adsorption equilibrium

Fig. 7 gives the results of equilibrium of chlorite adsorbed on MIEX resin at three different temperatures (293, 313, and 333 K). The adsorption capacity of chlorite onto MIEX resin increases with the temperature of solution being raised from 293 to 333 K. The higher temperature may activate some weak adsorption sites as well as decrease the viscosity of solution, causing the increase in adsorption capacity of chlorite adsorbed on MIEX resin with increasing temperature [46,47]. The increase in adsorption capacity with increasing temperature also indicates that the adsorption of chlorite on MIEX resin is an endothermic process in nature. Elevated temperature is beneficial to chlorite removal.

Quantitatively describing the adsorption equilibrium is significantly important for optimizing the use of adsorbent [48]. The equilibrium data of chlorite adsorbed on MIEX resin at different temperatures are examined by the Langmuir, Freundlich, and Redlich–Peterson (R–P) models, respectively. The three models can be described by Eqs. (7)–(9) [49,50]:

$$\text{Langmuir isotherm: } q_e = \frac{q_{\max} b C_e}{1 + b C_e} \tag{7}$$

$$\text{Freundlich isotherm: } q_e = k_f C_e^{\frac{1}{n}} \tag{8}$$

$$\text{R–P isotherm: } q_e = \frac{K_R C_e}{1 + a_R C_e^g} \tag{9}$$

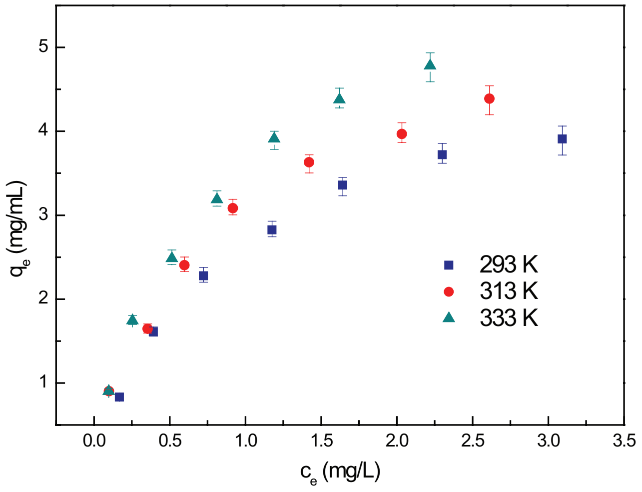

Fig. 7. Adsorption equilibrium of chlorite onto MIEX resin at different temperatures (the initial chlorite concentration = 1, 2, 3, 4, 5, 6, 7 mg/L; adsorbent dosage = 1.0 mL/L; agitation speed = 100 rpm; adsorption time = 90 min; pH without any adjustment).

where $q_{\max}$ (mg/mL) is the theoretical maximum adsorption capacity; b is a Langmuir isotherm constant related to the affinity of the binding; k_f (mg/mL (L/mg)$^{1/n}$) is the Freundlich constant related to the bonding energy and adsorption capacity; n is an empirical parameter related to the intensity of adsorption; K_R (L/mL), a_R (L /mg) and g are the R–P model parameters.

Table 2 shows that R–P isotherm model fits best to the equilibrium data of chlorite adsorbed on MIEX resin with the highest values of correlation coefficient (R^2 = 0.9872–0.9993) and the smallest values of SE = 0.45–2.04. Langmuir model assumes that the adsorption process occurs on a homogeneous surface, a monolayer adsorption of adsorbate, and no interaction among the adsorbed species. It is considerably difficult to completely satisfy these assumptions owing to the complexity of adsorption system. Hence the Langmuir model cannot well simulate the equilibrium of chlorite adsorbed on MIEX resin. Freundlich model mainly describes the heterogeneous or multi-layer adsorption behavior [51]. R–P isotherm model is a typical hybrid of Langmuir and Freundlich models. This may be a reason why the R–P isotherm model gives a good simulation. Although the Langmuir model does not give a best simulation to the equilibrium data, the theoretical maximum adsorption capacity ($q_{\max}$) obtained from Langmuir model is substantial for evaluating the performance of adsorbent as shown in Table 2 with $q_{\max}$ as 5.83 mg/mL.

3.7. Adsorption thermodynamics

Equilibrium data of chlorite adsorbed on MIEX resin at different temperatures were used to calculate the thermodynamics parameters. K_D (L/mL), the solid–liquid distribution coefficient at equilibrium, can be obtained by Eq. (10). Then the standard enthalpy change ($\Delta H°$, kJ/mol) and standard entropy change ($\Delta S°$, J/mol K) can be determined from the slopes and intercepts of the plots (presented in Fig. 8) of lnK_D against $1/T$ according to Eq. (11). And the standard Gibbs free energy change at different temperatures ($\Delta G°$, kJ/mol) can be calculated by Eq. (12) [52].

$$K_D = \frac{C_0 - C_t}{C_t} \times \frac{V}{W} \tag{10}$$

$$\ln K_D = \frac{\Delta S°}{R} - \frac{\Delta H°}{RT} \tag{11}$$

$$\Delta G° = \Delta H° - T\Delta S° \tag{12}$$

where R (8.314 J/mol K) is universal gas constant.

The negative $\Delta G°$ and positive $\Delta H°$ and $\Delta S°$ (listed in Table 3) show that the adsorption of chlorite on MIEX is a thermodynamically feasible, spontaneous, and endothermic process. Also, Table 3 demonstrates the values of $\Delta G°$ becoming more negative with an increase in temperature, revealing the adsorption is more spontaneous at high temperature.

3.8. Mechanism of chlorite adsorbed on MIEX resin

The kinetic data at the initial chlorite concentration of 5.57 mg/L were applied to analyze the concentration change of chlorite and chloride in solution with increasing the adsorption time, and the equilibrium data at 293 K were used to calculate the change in ion numbers of chlorite adsorbed on MIEX resin and chloride released into aqueous solution after equilibrium. Fig. 9 demonstrates the concentration of

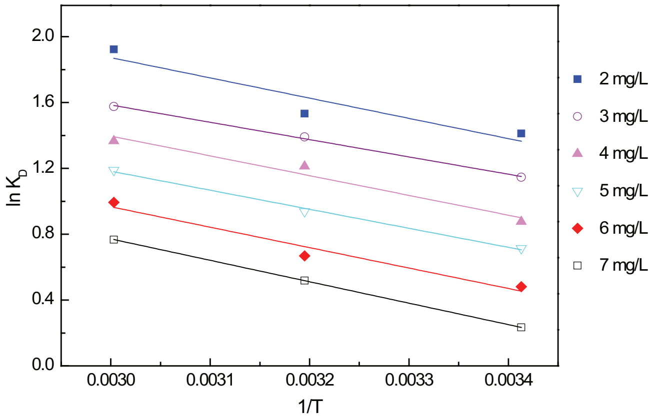

Fig. 8. Plots of lnK_D against $1/T$ for chloride adsorbed on MIEX resin.

Table 3
Thermodynamic parameters for chlorite adsorbed on MIEX resin

C_0 (mg/L)	$\Delta H°$ (kJ/mol)	$\Delta S°$ (J/mol K)	$\Delta G°$ (kJ/mol)		
			293 K	313 K	333 K
2	54.657	218.259	–9.293	–13.658	–18.023
3	34.279	143.076	–7.643	–10.504	–13.366
4	30.888	125.791	–5.969	–8.484	–11.000
5	25.082	102.204	–4.864	–6.908	–8.952
6	21.738	87.006	–3.755	–5.495	–7.235
7	18.013	71.833	–3.034	–4.471	–5.907

Table 2
Isotherm parameters for the removal of chlorite adsorbed on MIEX resin

T (K)	Langmuir model				Freundlich model				Redlich–Peterson model				
	$q_{\max}$ (mg/mL)	b (L/mg)	R^2	SE	k_f(mg mL (L/mg)$^{1/n}$)	$1/n$	R^2	SE	K_R (L/mL)	a_R (L/mg)	g	R^2	SE
293	5.03	1.177	0.9989	0.54	2.43	0.246	0.9696	2.90	6.022	1.226	0.978	0.9993	0.45
313	4.96	1.817	0.9659	3.33	2.92	0.500	0.9864	2.10	22.658	6.560	0.625	0.9872	2.04
333	5.83	1.641	0.9891	1.93	3.44	0.528	0.9890	1.94	15.026	3.265	0.715	0.9982	0.78

chloride in solution gradually increasing to an approximate constant value during the removal of chlorite, indicating that the ion-exchange reaction occurs. At the same time, it can be observed from Fig. 10 that the ion numbers of chlorite adsorbed on MIEX resin are appropriately equal to the ion numbers of chloride released into aqueous solution after equilibrium, verifying that the removal of chloride on MIEX resin is an ion-exchange mechanism.

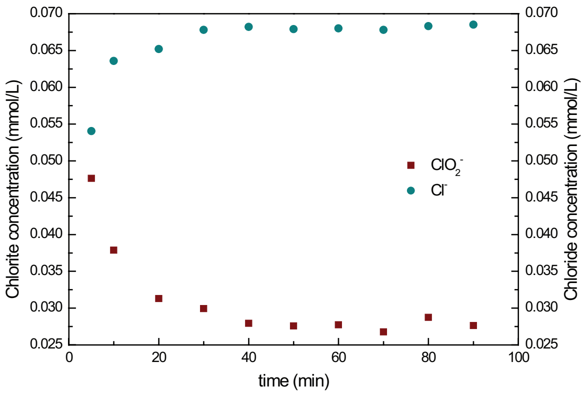

Fig. 9. Plots of chloride and chlorite ions concentration in solution vs. adsorption time.

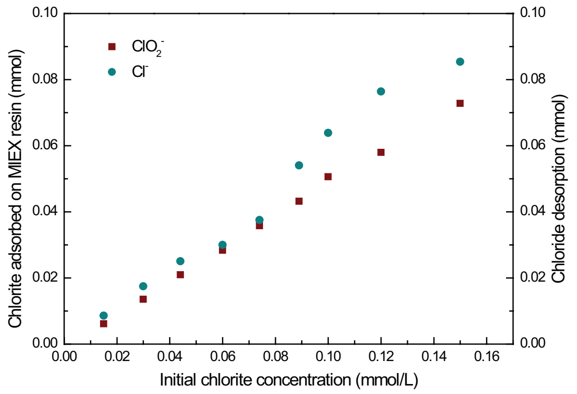

Fig. 10. Quantitative analysis of chlorite ions adsorbed on MIEX resin and chloride ions released into solution after adsorption equilibrium at 293 K.

3.9. Removal efficacy of chlorite in real water samples

Three real water samples are obtained from the effluents of sedimentation tanks at three different drinking water treatment plants where chlorine dioxide is used to pre-oxide the raw water. The water qualities before and after treatment by MIEX resin are listed in Table 4. The results show that for the tested water qualities, the MIEX dosage of 2 mg/L can reduce chlorite below the standard of 0.70 mg/L. In addition, Table 4 also shows that the DOC can be removed effectively as well as chlorite and chlorate. Therefore, MIEX resin is a promising technology for the removal of chlorite from aqueous solution.

4. Conclusions

The present study demonstrates that the MIEX resin is an effective adsorbent for the removal of chlorite from aqueous solutions. The agitation speed of 100 rpm can mix resin particles and aqueous solution quite well. The removal efficiency of chlorite increases with increasing dosage of MIEX resin. Under the tested conditions, the removal efficiency of chlorite keeps around 80% at the pH range of 5–7. The coexisting anions and NOM have significantly adverse impact on the removal of chlorite. The adsorption is a fast process, and equilibrium can be approximately attained within 40 min. The kinetics process of chlorite adsorbed on MIEX resin at the low chlorite concentration (1.02 mg/L) is highly possible to be pseudo-first-order. Conversely, the pseudo-second-order model can fit the kinetic data quite well at higher chlorite concentrations (2.28–5.57 mg/L). At the initial stage of adsorption, the intra-particle diffusion is the rate-controlling step. The adsorption rate is controlled by the film diffusion and the intra-particle diffusion after 10 min. The R–P isotherm model fits best to the equilibrium data. The adsorption is a thermodynamically feasible, spontaneous, and endothermic process. The removal of chloride on MIEX resin is an ion-exchange mechanism. The MIEX resin dosage of 2.0 mL/L can reduce chlorite in real water samples below the limited value of 0.7 mg/L.

Acknowledgments

This work was supported by the National Natural Science Foundation of China (grant number 51308001) and China Scholarship Council (201408340033).

Table 4
Water qualities before and after treatment by MIEX resin

Water sample	MIEX resin dosage (mL/L)		*T* (K)	Turbidity (NTU)	pH	ClO_2^- (mg/L)	ClO_3^- (mg/L)	Cl^- (mg/L)	SO_4^{2-} (mg/L)	DOC (mg/L)
1		Raw water	290.5	6.43	7.78	1.58	0.36	8.46	13.28	5.36
	1.0	Treated water	290.6	7.02	7.36	1.15	0.12	9.56	8.41	3.26
	2.0	Treated water	290.6	7.08	7.3	0.55	0.05	10.43	3.68	2.03
2		Raw water	290.3	5.84	8.03	0.96	0.48	8.23	15.02	6.54
	1.0	Treated water	290.3	6.16	7.48	0.72	0.33	9.62	8.78	4.38
	2.0	Treated water	290.3	6.28	7.28	0.32	0.11	10.28	4.69	2.69
3		Raw water	290.5	7.88	7.6	1.26	0.42	9.35	10.11	5.79
	1.0	Treated water	290.5	8.68	7.46	0.88	0.28	9.96	6.43	4.23
	2.0	Treated water	290.5	8.47	7.32	0.47	0.08	10.37	3.65	2.37

References

[1] S. Sorlini, M.C. Collivignarelli, M. Canato, Effectiveness in chlorite removal by two activated carbons under different working conditions: a laboratory study, J. Water Supply Res. Technol., 64 (2015) 450–461.

[2] X. Yang, W. Guo, W. Lee, Formation of disinfection byproducts upon chlorine dioxide preoxidation followed by chlorination or chloramination of natural organic matter, Chemosphere, 91 (2013) 1477–1485.

[3] S. Sorlini, C. Collivignarelli, Chlorite removal with granular activated carbon, Desalination, 176 (2005) 255–265.

[4] E. Righi, P. Bechtold, D. Tortorici, P. Lauriola, E. Calzolari, G. Astolfi, M.J. Nieuwenhuijsen, G. Fantuzzi, G. Aggazzotti, Trihalomethanes, chlorite, chlorate in drinking water and risk of congenital anomalies: a population-based case-control study in Northern Italy, Environ. Res., 116 (2012) 66–73.

[5] A. Katz, N. Narkis, Removal of chlorine dioxide disinfection by-products by ferrous salts, Water Res., 35 (2001) 101–108.

[6] M.W. Gill, M.S. Swanson, S.R. Murphy, G.P. Bailey, Two-generation reproduction and developmental neurotoxicity study with sodium chlorite in the rat, J. Appl. Toxicol., 20 (2000) 291–303.

[7] X. Zhang, R.J. Bull, J. Fisher, J.A. Cotruvo, B.S. Cummings, The synergistic effect of sodium chlorite and bromochloroacetic acid on BrO_3^--induced renal cell death, Toxicology, 289 (2011) 151–159.

[8] A. Hebert, D. Forestier, D. Lenes, D. Benanou, S. Jacob, C. Arfi, L. Lambolez, Y. Levi, Innovative method for prioritizing emerging disinfection by-products (DBPs) in drinking water on the basis of their potential impact on public health, Water Res., 44 (2010) 3147–3165.

[9] S.D. Richardson, M.J. Plewa, E.D. Wagner, R. Schoeny, D.M. DeMarini, Occurrence, genotoxicity, and carcinogenicity of regulated and emerging disinfection by-products in drinking water: a review and roadmap for research, Mutat. Res., 636 (2007) 178–242.

[10] H.B. Teh, S.F.Y. Li, Simultaneous determination of bromate, chlorite and haloacetic acids by two-dimensional matrix elimination ion chromatography with coupled conventional and capillary columns, J. Chromatogr., A, 1383 (2015) 112–120.

[11] G. Chen, H. Zhu, J. Qian, Study on the disinfection methods and disinfection by products control, Water Wastewater Eng., 40 (2014) 9–13.

[12] N. Gonce, E.A. Voudrias, Removal of chlorite and chlorate ions from water using granular activated carbon, Water Res., 28 (1994) 1059–1069.

[13] M.H. Griese, K. Hauser, M. Berkemeier, G. Gordon, Using reducing agents to eliminate chlorine dioxide and chlorite ion residuals in drinking water, J. Am. Water Works Assoc., 83 (1991) 56–61.

[14] M.H. Griese, J.J. Kaczur, G. Gordon, Combining methods for the reduction of oxychlorine residuals in drinking water, J. Am. Water Works Assoc., 84 (1992) 69–77.

[15] S. Sorlini, C. Collivignarelli, Chlorite removal with ferrous ions, Desalination, 176 (2005) 267–271.

[16] Y. Li, T.F. Xu, C.W. Cui, Y.X. Li, The adsorption of chlorite and chlorate by calcium carbonate in a drinking water pipe network, Desal. Wat. Treat., 53 (2015) 1881–1887.

[17] T.H. Boyer, P.C. Singer, A pilot-scale evaluation of magnetic ion exchange treatment for removal of natural organic material and inorganic anions, Water Res., 40 (2006) 2865–2876.

[18] K.A. Indarawis, T.H. Boyer, Superposition of anion and cation exchange for removal of natural water ions, Sep. Purif. Technol., 118 (2013) 112–119.

[19] J.N. Apell, T.H. Boyer, Combined ion exchange treatment for removal of dissolved organic matter and hardness, Water Res., 44 (2010) 2419–2430.

[20] B.A. Fil, A.E. Yilmaz, R. Boncukcuoğlu, S. Bayar, Removal of divalent heavy metal ions from aqueous solution by Dowex HCR-S synthetic resin, Bulg. Chem. Commun., 44 (2012) 201–207.

[21] S.K. Singh, T.G. Townsend, T.H. Boyer, Evaluation of coagulation ($FeCl_3$) and anion exchange (MIEX) for stabilized landfill leachate treatment and high-pressure membrane pretreatment, Sep. Purif. Technol., 96 (2012) 98–106.

[22] C.J. Johnson, P.C. Singer, Impact of a magnetic ion exchange resin on ozone demand and bromate formation during drinking water treatment, Water Res., 38 (2004) 3738–3750.

[23] T.H. Boyer, P.C. Singer, Bench-scale testing of a magnetic ion exchange resin for removal of disinfection by-product precursors, Water Res., 39 (2005) 1265–1276.

[24] M. Drikas, M. Dixon, J. Morran, Long term case study of MIEX pre-treatment in drinking water; understanding NOM removal, Water Res., 45 (2011) 1539–1548.

[25] P.A. Neale, M. Mastrup, T. Borgmann, A.I. Schafer, Sorption of micropollutant estrone to a water treatment ion exchange resin, J. Environ. Monitor., 12 (2010) 311–317.

[26] L. Ding, X. Lu, H.P. Deng, X.X. Zhang, Adsorptive removal of 2,4-dichlorophenoxyacetic acid (2,4-D) from aqueous solutions using MIEX resin, Ind. Eng. Chem. Res., 51 (2012) 11226–11235.

[27] P.C. Singer, K. Bilyk, Enhanced coagulation using a magnetic ion exchange resin, Water Res., 36 (2002) 4009–4022.

[28] H.-C. Kim, High-rate MIEX filtration for simultaneous removal of phosphorus and membrane foulants from secondary effluent, Water Res., 69 (2015) 40–50.

[29] S. Hsu, P.C. Singer, Removal of bromide and natural organic matter by anion exchange, Water Res., 44 (2010) 2133–2140.

[30] Y. Tang, S. Liang, H. Guo, H. You, N. Gao, S. Yu, Adsorptive characteristics of perchlorate from aqueous solutions by MIEX resin, Colloids Surf., A, 417 (2013) 26–31.

[31] Q. Wang, A. Li, J. Wang, C. Shuang, Selection of magnetic anion exchange resins for the removal of dissolved organic and inorganic matters, J. Environ. Sci., 24 (2012) 1891–1899.

[32] K.M. Walker, T.H. Boyer, Long-term performance of bicarbonate-form anion exchange: removal of dissolved organic matter and bromide from the St. Johns River, FL, USA, Water Res., 45 (2011) 2875–2886.

[33] L. Ding, H. Deng, C. Wu, X. Han, Affecting factors, equilibrium, kinetics and thermodynamics of bromide removal from aqueous solutions by MIEX resin, Chem. Eng. J., 181–182 (2012) 360–370.

[34] Y. Khambhaty, K. Mody, S. Basha, B. Jha, Kinetics, equilibrium and thermodynamic studies on biosorption of hexavalent chromium by dead fungal biomass of marine *Aspergillus niger*, Chem. Eng. J., 145 (2009) 489–495.

[35] S. Sobhanardakani, R. Zandipak, Z. Fili, M. Ghoochian, R. Sahraei, A. Farmany, Removal of V(V) ions from aqueous solutions using oxidized multi-walled carbon nanotubes, J. Water Supply Res. Technol., 64 (2015) 425–433.

[36] L.M. Liu, L. Li, Y.X. Zuo, Y.P. Huang, L.R. Song, Adsorption of 2-methylisoborneol and geosmin by a low-cost hybrid adsorbent synthesized from fly ash and bentonite, J. Water Supply Res. Technol., 60 (2011) 478–485.

[37] K.Y. Foo, L.K. Lee, B.H. Hameed, Batch adsorption of semi-aerobic landfill leachate by granular activated carbon prepared by microwave heating, Chem. Eng. J., 222 (2013) 259–264.

[38] M.A. Álvarez-Merino, M.A. Fontecha-Cámara, M.V. López-Ramón, C. Moreno-Castilla, Temperature dependence of the point of zero charge of oxidized and non-oxidized activated carbons, Carbon, 46 (2008) 778–787.

[39] K.S. Tong, M.J. Kassim, A. Azraa, Adsorption of copper ion from its aqueous solution by a novel biosorbent *Uncaria gambir*: equilibrium, kinetics, and thermodynamic studies, Chem. Eng. J., 170 (2011) 145–153.

[40] L. Ding, C. Wu, H. Deng, X. Zhang, Adsorptive characteristics of phosphate from aqueous solutions by MIEX resin, J. Colloid Interface Sci., 376 (2012) 224–232.

[41] N.Y. Mezenner, A. Bensmaili, Kinetics and thermodynamic study of phosphate adsorption on iron hydroxide-eggshell waste, Chem. Eng. J., 147 (2009) 87–96.

[42] E. Bulut, M. Özacar, İ.A. Şengil, Adsorption of malachite green onto bentonite: equilibrium and kinetic studies and process design, Microporous Mesoporous Mater., 115 (2008) 234–246.

[43] Ö. Aydın, C. Özmetin, M. Korkmaz, B.A. Fil, A semi-empirical kinetic model for removal of iron (Fe^{3+}) from saturated boric acid solution by ion exchange using Amberlite IR–120 resin, Part. Sci. Technol., (2015) (http://dx.doi.org/10.1080/02726351.2015.1076916).

[44] Y.-S. Ho, Review of second-order models for adsorption systems, J. Hazard. Mater., 136 (2006) 681–689.

[45] W.J. Weber, J.C. Morris, Kinetics of adsorption on carbon from solution, J. Sanit. Eng. Div. Proc. Am. Soc. Civ. Eng., 89 (1963) 31–59.

[46] F.W. Shaarani, B.H. Hameed, Ammonia-modified activated carbon for the adsorption of 2,4-dichlorophenol, Chem. Eng. J., 169 (2011) 180–185.

[47] C. Gong, Z. Zhang, Q. Qian, D. Liu, Y. Cheng, G. Yuan, Removal of bromide from water by adsorption on silver-loaded porous carbon spheres to prevent bromate formation, Chem. Eng. J., 218 (2013) 333–340.

[48] K.Y. Foo, B.H. Hameed, Insights into the modeling of adsorption isotherm systems, Chem. Eng. J., 156 (2010) 2–10.

[49] S.O. Kareem, A.I. Adeogun, S.O. Omeike, Biosorption studies for the removal of ferrous ion from aqueous solution by *Aspergillus terreus* and *Trichoderma viride*: kinetic, thermodynamic and isothermal parameters, J. Water Supply Res. Technol., 63 (2014) 66–75.

[50] B.A. Fil, R. Boncukcuoğlu, A.E. Yılmaz, S. Bayar, Adsorption kinetics and isotherms for the removal of zinc ions from aqueous solutions by an ion-exchange resin, J. Chem. Soc. Pak., 34 (2012) 841–848.

[51] A.E. Yilmaz, B.A. Fil, S. Bayar, Z.K. Karakaş, A new adsorbent for fluoride removal: the utilization of sludge waste from electrocoagulation as adsorbent, Global NEST J., 17 (2015) 186–197.

[52] B.A. Fil, A.E. Yilmaz, S. Bayar, Adsorption of Ni(II) on ion exchange resin: kinetics, equilibrium and thermodynamic studies, Korean J. Chem. Eng., 29 (2012) 1232–1238.